Nasal characteristics in patients with asymmetric mandibular prognathism

Yi Fan[1,2,3], Gui Chen[1,2], Wei He[4], Nan Zhang[1,2,] Guangying Song[1,2], Harold Matthews[3,5,6], Peter Claes[3,5,6,7], Tianmin Xu[1,2]

1. Department of Orthodontics, Peking University School and Hospital of Stomatology, Beijing, China
2. National Engineering Laboratory for Digital and Material Technology of Stomatology, Beijing Key Laboratory of Digital Stomatology, Peking University School and Hospital of Stomatology, Beijing, China
3. Facial Science, Murdoch Children's Research Institute, Melbourne, Australia
4. Department of Oral and Maxillofacial Surgery, Peking University School and Hospital of Stomatology, Beijing, China
5. Department of Human Genetics, KU Leuven, Leuven, Belgium
6. Medical Imaging Research Centre, Universitair Ziekenhuis, Leuven, Belgium
7. Department of Electrical Engineering, KU Leuven, Leuven, Belgium

Co-first authors:
Yi Fan and Gui Chen are co-first authors.

Corresponding authors:
Tianmin Xu
E-mail: tmxuortho@163.com
Phone: 010-82195330

Address: Peking University School and Hospital of Stomatology
No.22, Zhongguancun South Avenue Haidian District, Beijing, 100081, China

Nasal characteristics in patients with asymmetric mandibular prognathism

Abstract:

Aims: To objectively quantify nasal characteristics of patients with asymmetric mandibular prognathism and to evaluate the association between nasal asymmetry and dentofacial abnormalities. **Methods:** Ninety adult patients with asymmetric mandibular prognathism were included. Images were captured pre-treatment using three-dimensional stereo-photogrammetry. 7,160 uniformly sampled quasi-landmarks were automatically identified on each facial image to establish correspondence using a template mapping technique. 15 commonly used anatomical landmarks were then automatically located on each image though barycentric to Cartesian coordinates conversion. Nasal characteristics and asymmetry were quantified by anthropometric linear distances and angular measurements as well as surface-based analysis. The degree of nasal, chin and peri-orbital asymmetry in an individual were scored using a root-mean-squared-error between the left and right sides. The correlations among these regional asymmetries were evaluated. **Results:** The nasal tip was significantly shifted to the deviated side of the chin and the nostrils were asymmetrical. The location and degree of nasal asymmetry varied among patients with asymmetric mandibular prognathism. The level of nasal asymmetry was significantly and positively correlated with chin asymmetry and peri-orbital asymmetry. **Conclusion:** Nasal asymmetry is present in asymmetric mandibular prognathism patients. Furthermore, it is positively associated with peri-orbital deviation and chin deviation. Individualized nasal asymmetry evaluation should be performed, and clinicians should inform patients preoperatively about preexisting nasal asymmetry.

Key Words: nasal asymmetry, chin deviation, automatic landmark indication, 3D facial imaging

Introduction

Facial asymmetry is frequently seen in patients with skeletal malocclusion, especially those with asymmetric mandibular prognathism.[1-3] The lateral deviation of chin is usually the most noticeable feature in these patients. It has also been reported that nasal asymmetry, including nasal bridge and alar base deviation; perioral asymmetry, including lip-line cant; and philtrum deviation accompany asymmetric mandibular prognathism.[4,5]

Orthognathic surgery is a recognized method of correcting dentofacial deformities. It is common practice to treat problems that affect the chin simultaneously, while deferring or not treating nasal deformities.[6] Many dentofacial deformity patients, who present with a principal complaint of chin deviation, are unaware of other preexisting asymmetry. Therefore, recognizing and discussing the interrelations among the deviated nose and other facial structures is an important consideration in surgical planning. To date, there is inadequate published information about the nasal characteristics of patients with asymmetric mandibular prognathism, and the association between dentofacial and nasal deformities in these patients.

Commonly used soft tissue nasal measurements include (1) direct anthropometric measurements by rulers or calipers,[7] (2) photogrammetric measurements,[4,8] (3) optical measurements,[9] (4) three-dimensional (3D) photos or computed tomographic (CT) measurements.[4] The accuracy of

direct measurements largely relies on the clinician's skill. Facial photographic analysis, which assesses changes to the nose from 2D images, can be erroneous. Factors causing this include unstandardized head postures of the photographed patients; magnification differences between cameras and imaging protocols; and geometric distortion caused by projection of the 3D structure to a 2D plane. [10] 3D photos or CT images allow for conventional measurements such as distances or angles to be taken, while preserving information on the 3D size and shape of the nasal structures. Commonly used anthropometric analyses yields reliable and reproducible results after repeat measurements. However, big data initiatives are increasingly common in dentistry and surgical disciplines. To process large numbers of medical images requires fast, automated, and standardized landmark indications and measurements. Several automatic landmark indications algorithms have been suggested in the literature. [11-14] However, these have rarely been applied to patient evaluations.

Therefore, the aim of this study was to apply an automatic landmark indication technique to quantify the nasal characteristics in subjects with asymmetric mandibular prognathism. In addition, we assess the correlations among nasal asymmetry, chin asymmetry and peri-orbital asymmetry in these patients.

Methods

Patients

This retrospective study included 90 patients (32 males and 58 females; Age: 20.90 ± 3.94 years (mean ± SD); ANB: -3.60° ±2.45° (mean ± SD)). We selected patients who seek for combined surgical-orthodontic treatment to correct for dentofacial deformity at [redacted]. These patients were consecutively treated with at least a combined Le Fort I and a bilateral sagittal split osteotomy with either traditional orthognathic surgery or surgery-first approach. The inclusion criteria were 1) Chinese adult patients aged 18 -35 years of age; 2) skeletal Class III malocclusion with mandibular prognathism. 3)Asymmetric mandibular prognathism was defined by clinically diagnosed asymmetry of the lower face and Menton deviation from the midsagittal reference line evaluated on CBCT images during pre-surgical assessment. Patients with other congenital anomalies or a history of maxillofacial trauma or surgery were excluded. Statistical power at the available sample sizes was estimated using the 'pwr' package in R. All calculations assume a two-tailed p value and a type I error rate of .05. For the independent-samples t-tests between males and females we have >=80% power to detect a difference, where the effect size (Cohen's D) is >=.624. For the paired samples t-test comparing left and right measurements we have >=80% power to detect a difference where the effect size (Cohen's D) is >=.298. For the correlation analyses we have >80% power to detect a correlation when the effect size (Spearman's rho)>=.29. The study was approved by the Institutional Review Board of [redacted]. All participants provided written informed consent before participation.

Facial image acquisition

3D images were captured using the 3dMD imaging system (3dMD Inc, Atlanta, Ga). Patients were instructed to maintain a neutral facial expression in their natural head position when scanned, with

lips and mouth at rest and teeth in intercuspation to minimize involuntary movement.[15] Each facial image comrpises a polygonal surface defined in 3D coordinate space.

Automatic facial quasi-landmarking

Facial images in .obj format were imported into the MeshMonk toolbox of MATLAB (R2019b) for spatially dense facial quasi-landmarking.[14] This process automatically identified the same set of dense points on each facial image. Briefly, an anthropometric mask (the template), represented by 7,160 quasi-landmarks, was firstly rigidly align to each target face. Then the anthropometric mask was deformed to each the target face (Fig 1). This resulted in 7,160 quasi-landmarks that capture the entire facial region while removing irrelevant structures such as hair, ears, shoulders and any irrelevant polygons.

Automatic identification of nasal landmarks

Because the registered faces were represented by the same points as the template, we could subsequently transfer manual landmarks indicated on the template to each registered face following a barycentric to Cartesian coordinates (x,y,z co-ordinates) conversion.[14,16] In this study, two independent observers placed 15 anatomical landmarks (Table 1) twice each on the pre-registered template, with at least 24 hours in between landmarking sessions, resulting in four landmark indications. Intra- and interobserver reproducibility was calculated by means of intraclass correlation coefficient (ICC). The mean ICC for intra-observer reproducibility was 0.998 (min:0.997, max:0.999). The mean ICC for inter-observer reproducibility was 0.997 (min:0.996, max:0.998). The average of all four manual landmark indications was used as the final manual landmark indication on the pre-registered template. As these average landmarks were not always exactly located on the surface, they were first projected onto the nearest triangular facet of the template. The automatic landmarking process is illustrated in Fig 2. Cartesian coordinates are commonly known x, y, z coordinates of a point in three-dimensions, which specify the signed distance from the origin along the x, y and z-axes, respectively. Three corresponding quasi-landmarks, defined by the Cartesian coordinates, compose of three vertices (corners) of a triangle ABC. Barycentric coordinates define any point inside a triangle by assigning weights (λ) to each of the triangle vertices in a manner that the weighted average of the vertices equals the coordinates of that specific point. For example, the position of the Pronasale (Prn) inside the triangular facet ABC is coded as barycentric co-ordinates. These are weights on each vertex of the triangle such that the weighted average of the Cartesian co-ordinates of triangle vertices equals the Cartesian coordinates of Prn. To find the Cartesian co-ordinates of landmark Prn' on any target face, we calculate the weighted average of vertices A'B'C' on the target face, which structurally corresponds to triangle ABC on the template, but with different Cartesian coordinates due to the difference in the size, shape and location of the faces. In this way, the 15 manually indicated facial anatomical landmarks were automatically placed on all 90 subjects to be evaluated in this study.

Anthropometric analysis

The anthropometric measurements that quantified the asymmetry of the nose included (Fig 3):

1) Alare - En-En distance (Al-En): the vertical distances from the right and left alare to the intercanthal line. The left and right sides of this index reflect the alare deviation.

2) Alar curvature point - En-En distance (Ac-En): the vertical distances from the right and left alar curvature points to the intercanthal line. The left and right sides of this index reflect the alar base deviation.
3) Pronasale - alar distance (Prn-Al): The distances from the pronasale to the bilateral alare. The left and right sides of this index reflect the deviation of the nasal tip.
4) Columella - alar curvature point distance (C'-Ac): the distance from columella to bilateral alar curvature points. The left and right sides of this index reflect the columella deviation.
5) Nostril axis angle: the angle at the intersection of the line from the uppermost point to the lowermost point of the nostril and the Ac-Ac line. The left and right comparison of this index can reflect the differences in the long axis and morphology of the bilateral nostrils.

Anthropometric measurements were compared between the chin deviated side and the non-deviated side. The mean left-right difference between nasal measurements were compared between males and females.

Surface-based analysis and visualization

Surfaced-based analysis was performed to quantify and visualize the overall nasal asymmetry. This was achieved by superimposing the original 3D facial image and its mirror copy. The difference between corresponding points on the original and mirror copy was visualized as a color-coded map. Briefly, the template mapping was applied to each original and mirror image (created by reversing the sign of the x-co-ordinate of each point on the original). Then, the robust Procrustes superimposition was used to superimpose the original face and the mirror face.[16,17] This transformation was recorded. The distance at each point (in mm) between each original and mirror face was visualized on the original configuration as a color map. The nasal asymmetry index, chin asymmetry index and the peri-orbital asymmetry index for each patient was obtained by calculating the root mean square of the distances between original and reflected images of the quasi-landmarks occupying the specific anatomical regions (errors; RMSE).[17] As a byproduct of the protocol an estimate of the midsagittal plane was then obtained by: 1) reflecting the quasi-landmark configuration of the original image 2) then applying the previously estimated Procrustes transformation to this mirror configuration and 3) fitting a plane through the midpoints between each corresponding point on the original quasi-landmark configuration and the mirrored and aligned quasi-landmark configuration. The deviated side of the chin was determined by measuring the soft tissue Menton position relative to the midsagittal plane. All the analysis was performed using custom-written code in the Python programming language.

Statistical Analysis

Statistical analysis was performed using SPSS software for Windows (version 17.0; SPSS Inc). Differences in the linear, angular and area measurements between deviated and non-deviated sides was assessed using a paired t-test between double measurements. When the requirement of normality failed; Wilcoxon signed ranks test was used to assess the significance of the differences for matched pairs. Sexual dimorphism of the nasal asymmetry was evaluated by comparison the differences of the nasal parameters. The association between nasal asymmetry, periorbital asymmetry and chin asymmetry were evaluated by Spearman rank order correlation coefficient. Statistical significance was set at $P < .05$.

Results

Anthropometric measurements

The means and standard deviations of the nasal parameters were compared between the chin-deviated side and non-deviated side in mandibular prognathism patients (Table 2). The mean value of the pronasale- alar distance was shorter in the deviated side than the non-deviated side, indicating significant nasal tip deviation. The nostril axis angle was also significantly different between the two sides. Other nasal parameters were not significantly different between the two sides.

Table 3 shows the mean and SD of the differences between corresponding left and right-side measurements, for males and females. The final column is the p value of an independent samples t-test comparing the mean of males to females. The results indicated that there were no statistically significant differences of nasal asymmetry between males and females in this cohort.

Surface-based measurements and the association between the asymmetries

Ten patients with the highest nasal asymmetry index were selected to be visualized using a color coded map (Fig 4). Red areas indicate regions where the asymmetry was larger than 4mm and dark blue areas indicate no asymmetry. A high degree of nasal asymmetry was present in mandibular prognathism patients especially those with severe chin deviation. The location and severity of the nasal asymmetry varied.

The median for nasal asymmetry index was 1.75, (range, 0.77 to 4.71). The median for peri-orbital asymmetry index was 1.95 (range, 0.84 to 5.44). The median for chin asymmetry index was 2.41 (range, 0.97 to 12.52). Figure 5 shows the relationship among these asymmetries across the whole spectrum of asymmetry values that are present within our data. The Spearman rank order correlation coefficient revealed nasal asymmetry was significantly positively correlated with chin asymmetry and periorbital asymmetry (Table 4).

Discussion

In the present study, we evaluate nasal characteristics of patients with asymmetric mandibular prognathism. A large amount of nasal asymmetry was detected, and the location and degree of nasal asymmetry varied. The nasal tip was significantly shifted to the deviated side of the chin and the nostrils were asymmetrical before orthodontic and orthognathic surgery treatment. In addition, a high level of nasal asymmetry is associated with a high level of periorbital asymmetry and chin deviation.

The nose is located in the middle of the face and is recognized as a crucial factor in determining facial attractiveness. Orthodontic, combined with orthognathic surgery is the recognized treatment for dentofacial deformities with the key goals of correcting malocclusion and improving facial aesthetics. In our daily practice, we frequently encounter patients with a deviated chin who are unaware of their accompanying facial asymmetry in other facial anatomical regions. Orthodontists and surgeons often find that, despite their best efforts to straighten the teeth and jaws, patients quite often perceive their nose and muscles as being deviated, and this observation is more

prevalent in patients with asymmetric mandibular prognathism. However, there is inadequate published information that objectively quantifies the nasal deformities in these patients.

Many genetic and environmental factors can affect nasal aesthetics. The nasal septal cartilage and its bilateral triangular cartilage roughly form a T-shaped rod, which is partially covered by the nasal bone. Some scholars believe that the T-shaped cartilage structure of the nose is growing and constantly changing throughout life.[18] The growth and adaptation of nasal cartilages are progressive and related to the growth of the middle third of the face.[19] When there are facial deformities, the maxilla and mandible are frequently involved, so it is to be expected that in such a case the nose is also a component in the deformity.[4]

In this study, a large amount of nasal asymmetry was detected in patients presenting with asymmetric mandibular prognathism. This is consistent with the finding of Olate et al. that almost 50% of the patients with Class III dentofacial deformities also present with nasal deformities.[4] By measuring various components of the nose, we showed that significant nasal tip deviation and nostril asymmetry are present in asymmetric mandibular prognathism patients. As the patients usually pay more attention to their facial appearance after surgery, information on preexisting nasal asymmetry should be provided to patients with mandibular chin deviation. In addition, previous literature has shown that maxillary advancement can result in raising/rotating the nasal tip, widening the alar base, and lowering the columella.[4,6,20] Therefore, nasal changes that accompany maxillary osteotomies should be taken into consideration when planning orthognathic surgery and patients should be notified of these potential risks preoperative. In addition, postoperative rhinoplasty could be suggested in order to achieve facial harmony.

According to our correlation analysis, nasal deviation was significantly positively correlated with chin asymmetry. This agrees with findings in previous studies that mandibular chin deviation was accompanied by nasal deviation.[5] However, this is not necessarily indicative of any developmental relationship between the two structures as the mandibular process grows separately from the nasal component. Therefore, it is more likely that the nasal asymmetry is a result of overall compensation of the facial soft tissue, which consists of slanting of the whole face to one side according to clinical observation. Furthermore, nasal deviation showed an even stronger correlation with periorbital asymmetry. Embryologically, the nose originates from the frontonasal prominence, developing by local thickenings of the surface ectoderm. The maxillary prominence, a tissue of mesodermal origin, derives from the first branchial arch. These two structures are closely related to each other and the development of the nose is completed by the fusion of the frontonasal and maxillary processes.[5] This explains the potential reciprocal effect of nasal and maxillary complex growth and the high level of correlation between the asymmetry of these two structures.

Previously, nasal characteristics have been quantified by 2D photographic measurements, which do not accurately represent the full 3D anatomy. The rapid increase in the availability of 3D scanning devices has moved facial analysis into the 3D domain. 3D facial landmarks are often used as simple measures of anatomy. It is crucial to have accurate algorithms for automatic landmark placement because manual landmark indication is tedious, time-consuming and could

introduce inter- and intra-operator errors. In contrast to major reports using manually indicated nasal landmarks on the images,[4,21] we applied a previously validated facial landmarking method developed by our group to automatically identify facial landmarks on mandibular prognathism patients. The landmarks are placed by computing the correspondence between a template face and any given face with a computer algorithm, allowing for large number of faces to be analyzed quickly. Moreover, the location and severity of nasal asymmetry is intuitively visualized by a color-map by superimposing the corresponding points correspondence instead of the closet point correspondence, which is widely used in Iterative Closest Point (ICP) algorithm. The ICP approximates each point on one surface as its nearest neighbor on the other surface which is incorrect when dealing with severely asymmetric cases.[17,22] We establish the correspondence by updating ‘closeness’ points as the template gradually changes its shape, ensuring that anatomically meaningful correspondence is established at the end of the algorithm. After superimposing the original and mirror face, the accuracy of the correspondences determines the accuracy of the asymmetry assessment. Individualized visualization of the asymmetry offers a tool for improving patient communication, education and individualized treatment planning.

The limitation of this study is 3D facial images of Chinese general population are not available. Slight nasal asymmetry that is similar to what we see in the general population may mix in the sample. It would be helpful to include a control group in future study to delineate a true relationship of nasal asymmetry to other dentofacial asymmetries. Furthermore, the etiology of the nasal asymmetry in asymmetric mandibular prognathism and surgical impact on nasal asymmetry remains unclear. Post-operative 3D photographs should be collected to identify the treatment effect and additional nasal deformities introduced by maxillary osteotomies.

Conclusion

In conclusion, nasal asymmetry is present in asymmetric mandibular prognathism patients. Nasal asymmetry is positively associated with periorbital deviation and chin deviation. We recommend that individualized nasal asymmetry evaluation be performed, and clinicians inform patients preoperatively about preexisting nasal asymmetry. In contrast to focusing on only the chin, increasing patient awareness of asymmetries over the whole face, including nasal asymmetry, will provide greater patient satisfaction in their surgical outcomes.

Conflict of interest statement

The authors declare that there is not any conflict of interest in conducting this study.

Funding

This work was supported by [redacted]

References

1. Hågensli N, Stenvik A, Espeland L. Asymmetric mandibular prognathism: Outcome, stability and patient satisfaction after BSSO surgery. A retrospective study. J Cranio-Maxillofacial Surg 2014;42:1735–41.

2. Kamata H, Higashihori N, Fukuoka H, Shiga M, Kawamoto T, Moriyama K. Comprehending the three-dimensional mandibular morphology of facial asymmetry patients with mandibular prognathism. Prog Orthod 2017;18:43.
3. Duran GS, Dindaroğlu F, Kutlu P. Hard- and soft-tissue symmetry comparison in patients with Class III malocclusion. Am J Orthod Dentofac Orthop 2019;155:509–22.
4. Olate S, Cantín M, Muñoz M, Alister JP, Vásquez B, Chaves Netto H. Nasal deformity in subjects with class III facial deformities. Int J Morphol 2015;33:1536–41.
5. Shin Y-M, Lee S-T, Nam K-Y, Kwon T-G. Nasal deviation in patients with asymmetric mandibular prognathism. J Craniofac Surg 2017;28:e700–4.
6. Seah TE, Bellis H, Ilankovan V. Orthognathic patients with nasal deformities: Case for simultaneous orthognathic surgery and rhinoplasty. Br J Oral Maxillofac Surg 2012;50:55–9.
7. LG Farkas. Asymmetry of the head and face. In: Anthropometry of the head and face-2-nd edition. 1997. p. 7,103.
8. Hafezi F, Naghibzadeh B, Nouhi A, Yavari P. Asymmetric facial growth and deviated nose: A new concept. Ann Plast Surg 2010; 64:47–51.
9. Burke PH. Serial observation of asymmetry in the growing face. Br J Orthod 1992;19:273–85.
10. Park SB, Yoon JK, Kim Y Il, Hwang DS, Cho BH, Son WS. The evaluation of the nasal morphologic changes after bimaxillary surgery in skeletal class III maloccusion by using the superimposition of cone-beam computed tomography (CBCT) volumes. J Cranio-Maxillofacial Surg 2012;40:e87–92.
11. Ruiz MC, Illingworth J. Automatic landmarking of faces in 3D. In: 5th International Conference on Visual Information Engineering (VIE 2008). IEE 2008. p. 41–6.
12. Wei R, Claes P, Walters M, Wholley C, Clement J. Augmentation of linear facial anthropometrics through modern morphometrics: a facial convexity example. Aust Dent J 2011;56:141–7.
13. Torosdagli N, Liberton DK, Verma P, Sincan M, Lee JS, Bagci U. Deep geodesic learning for segmentation and anatomical landmarking. IEEE Trans Med Imaging. 2019;38:919–31.
14. White JD, Ortega-Castrillón A, Matthews H, Zaidi AA, Ekrami O, Snyders J, et al. MeshMonk: Open-source large-scale intensive 3D phenotyping. Sci Rep 2019;9:6085.
15. Tian K, Li Q, Wang X, Liu X, Wang X, Li Z. Reproducibility of natural head position in normal Chinese people. Am J Orthod Dentofac Orthop 2015;148:503–10.
16. Ekrami O, Claes P, White JD, Zaidi AA, Shriver MD, Van Dongen S. Measuring asymmetry from high-density 3D surface scans: An application to human faces. PLoS One 2018;26;13:e0207895.
17. Claes P, Walters M, Vandermeulen D, Clement JG. Spatially-dense 3D facial asymmetry assessment in both typical and disordered growth. J Anat 2011;219:444–55.
18. ML Moss. The primacy of functional matrices in orofacial growth. Dent Pract Dent Rec 1968;19:65–73.
19. D'Ascanio L, Lancione C, Pompa G, Rebuffini E, Mansi N, Manzini M. Craniofacial growth in children with nasal septum deviation: A cephalometric comparative study. Int J Pediatr Otorhinolaryngol. 2010;74:1180–3.
20. Dantas WRM, da Silveira MMF, do Egito Vasconcelos BC, Porto GG. Evaluation of the nasal shape after orthognathic surgery. Braz J Otorhinolaryngol 2015;81:19–23.
21. Funayama E, Yamamoto Y, Oyama A, Furukawa H, Murao N, Hayashi T, et al. Comparison of

nasal symmetry between presurgical nasal stenting and postsurgical nasal retainer placement in unilateral clefts. J Craniofac Surg. 2019;30:133–6.

22. Xiong Y, Zhao Y, Yang H, Sun Y, Wang Y. Comparison between interactive closest point and Procrustes analysis for determining the median sagittal plane of three-dimensional facial data. J Craniofac Surg. 2016;27:441–4

Figure legend

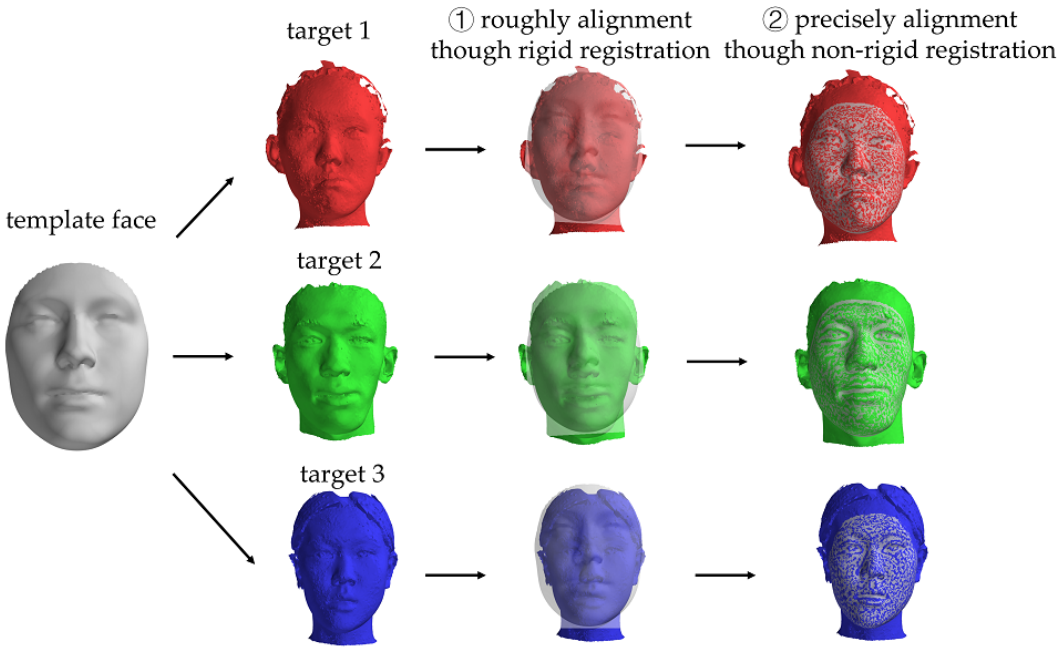

Fig 1. Template mapping. The template roughly aligns to each target face through rigid registration (translation, rotation and scale) and then deforms to match precisely to each target face through non-rigid registration.

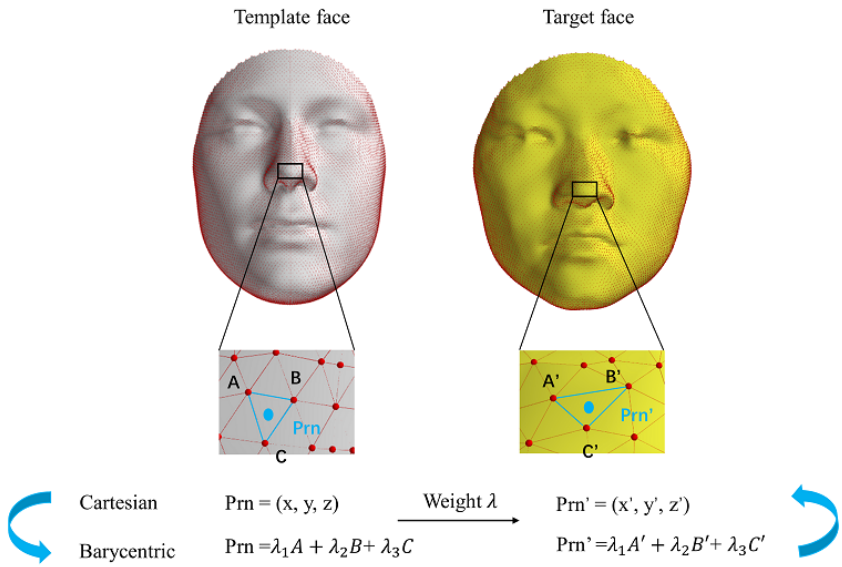

Fig 2. Barycentric coordinates to landmark coordinates conversion. The barycentric coordinates of point Pronasale (Prn) are calculated with respect to triangle ABC on the template face. The barycentric weights (λ) is calculated and applied to triangle A'B'C on the target face, which structurally corresponds to triangle ABC on the template, but with different Cartesian coordinates due to the difference in the shape of the faces.

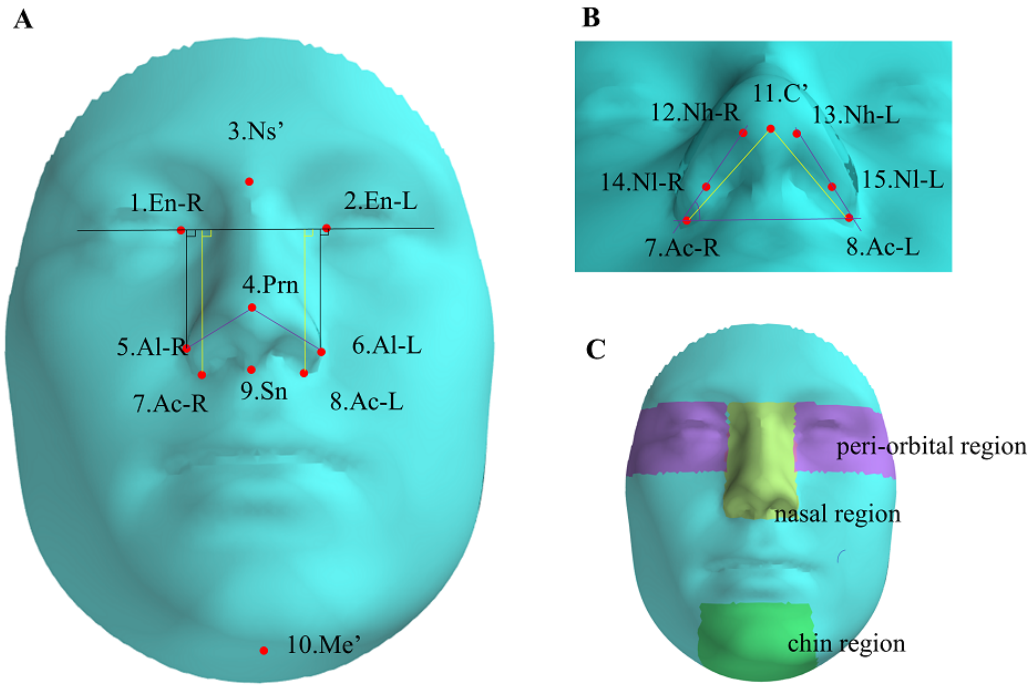

Fig 3. A and B: Linear distance and angular measurements of the nose. 1. right endocanthion (En-R); 2. left endocanthion (En-L); 3. soft tissue nasion (Ns'); 4. pronasale (Prn); 5. right ala (Al-R); 6. left ala (Al-L); 7. right alar curvature point (Ac-R); 8. left alar curvature point (Ac-L); 9. subnasale (Sn); 10. soft tissue menton (Me'); 11. columella (C'); 12. highest point of right nostril (Nh-R); 13. highest point of left nostril (Nh-L); 14. lowest point of right nostril (Nl-R); 15. lowest point of left nostril (Nl-L). **C:** facial regions.

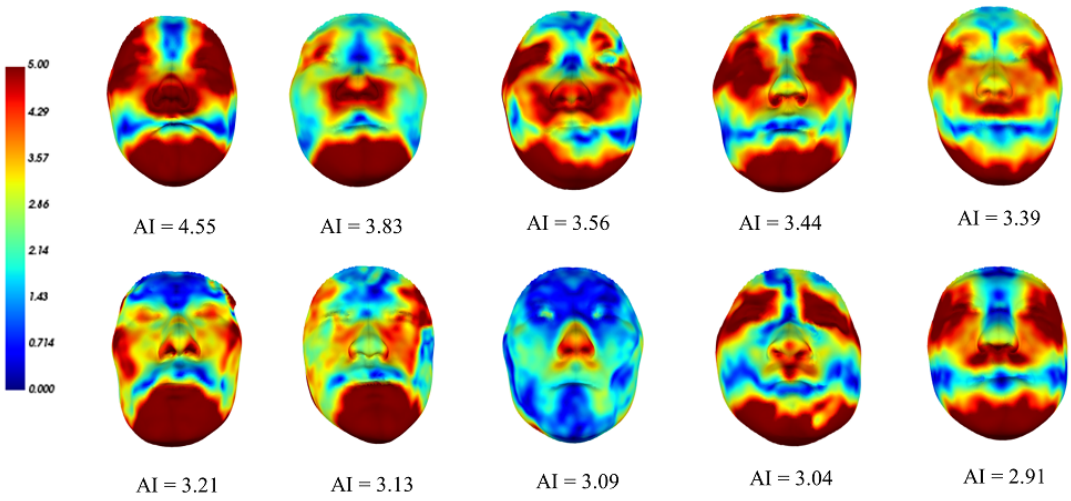

Fig 4. Color-map visualization of the nasal asymmetry.

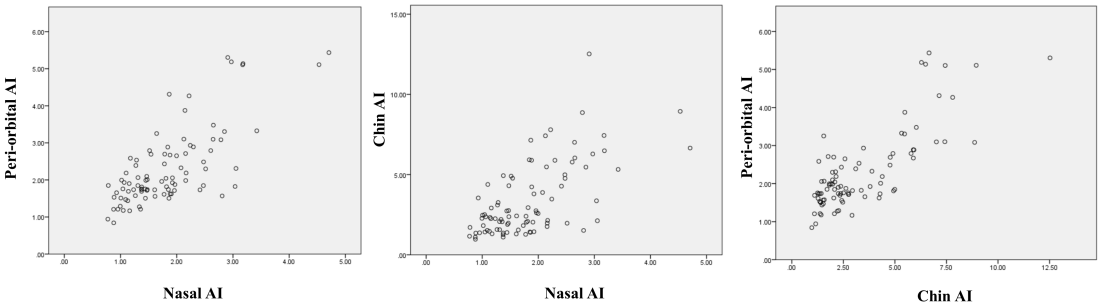

Fig 5. Scatter plots for the association among nasal asymmetry, peri-orbital asymmetry and chin asymmetry.

Table 1. Facial anatomical landmarks

Name	Abbreviation	Definition
Endocanthion	En (R,L)	Point at the inner commissure of the eye fissure
Soft tissue nasion	N	The midpoint on the soft-tissue contour of the base of the nasal root
Pronasale	Prn	The most protruded point of the nasal tip
Subnasale	Sn	The midpoint of the angle at the columella base where the lower border of the nasal septum and the surface of the upper lip meet
Alare	Al(R,L)	The most lateral point on each alar contour
Alar curvature point	Ac(R,L)	The most lateral point in the curved baseline of each ala indicating the facial insertion of the nasal wingbase
Columella apex	C'	The most anterior, or the highest point on the columella crest at the apex of the nostril
Subnasale	Sn	The midpoint on the columella crest that transects the lines connecting apices of the nares
Highest point of nostril	Nh(R,L)	The highest point of the nostril
Lowest point of nostril	Nl(R,L)	The lowest point of the nostril
Soft tissue menton	Me’	Most inferior midpoint of the soft tissue chin

Table 2. Nasal parameters comparison between the chin deviated side and the non-deviated side

Measurements	Chin deviated side (mean ±SD)	Chin non-deviated side (mean ±SD)	Difference (mean ±SD)	P-value*
Al-En	40.46 ± 2.51	40.45 ± 2.62	0.01 ± 1.24	0.919
Ac-En	46.64 ± 2.64	46.69± 2.70	-0.04 ± 1.04	0.717
Prn-Al	24.93± 1.82	25.22 ± 1.85	-0.29 ± 0.99	0.007 *
C'-Ac	21.15 ± 1.48	21.08 ± 1.60	0.07 ± 0.87	0.441
Nostril axis angle	55.61 ±6.27	59.30 ± 5.79	-3.69 ± 9.10	<0.001 ** †

*Paired t tests between the two sides in each group; † Wilcoxon signed ranks test was used because the difference between the two sides had non-normal distribution.

Table 3. Gender comparison between corresponding left and right-side nasal measurements

Measurement	Males (mean ±SD)	Females (mean ±SD)	Independent t-test P-value
Diff(Al-En)	0.99 ± 0.94	0.96 ± 0.67	0.87
Diff(Ac-En)	0.87 ± 0.84	0.74 ± 0.58	0.46
Diff(Prn-Al)	0.86 ± 0.59	0.81± 0.61	0.70
Diff(C'-Ac)	0.77 ± 0.61	0.62 ± 0.51	0.21
Diff(Nostril axis angle)	8.91 ±3.14	9.26 ± 0.67	0.65

Table 4. The association between nasal asymmetry, periorbital asymmetry and chin asymmetry using Spearman's rank correlation test

		Nasal AI	Peri-orbital AI	Chin AI
Spearman's rank correlation coefficient P-values	Nasal AI	1.000	0.664** <0.001	0.587** <0.001
	Peri-orbital AI	0.664** <0.001	1.000	0.675** <0.001
	Chin AI	0.587** <0.001	0.675** <0.001	1.000